JOURNAL NAME: Journal of Membrane Science & Technology

MANUSCRIPT NUMBER: JMST-2020-21

ISSN NUMBER: 2155-9589

ARTICLE TYPE: Research Article

Using Activated Charcoal for Decrease Iron, Fluoride, Phosphate, COD and TSS from Wastewater of phosphate fertilizer plant

M.S. Abdel Zaher[1*], S.M. Abdel Wahab[2], M.H. Taha[3], A. M. Masoud[3]

*[1]*Abu Zaabal Fertilizer & Chemical Company; [2]Department of Chemistry, Faculty of Science, Ain Shams University, Cairo, Egypt; [3]Nuclear Materials Authority, El Maddi, Cairo, Egypt*

ABSTRACT

Phosphate fertilizer industries produce a certain type of high acidity liquid (pH = 2) and contain large amounts of contaminants such as fluoride, phosphates and other elements. The high content of these pollutants and the massive daily flow rate of waste water produced by the fertilizer industry from phosphoric acid and / or the production of triple superphosphate (TSP) results in the discharge of several thousand tons of these elements annually. Waste samples were acquired from wastewater streams produced in Abu Zaabal for Fertilizer and Chemicals Company (AZFC). The present study intelligences a process for iron, fluoride, phosphate, COD and TSS sorption from the wastewater samples using activated charcoal. Accordingly, a series of batch experiments were achieved to study the effect of several experimental parameters, such as solution shaking time, solution pH, and clay amount of addition, temperature, and mechanical stirring speed. The obtained results clear that, the sorption preferred conditions were; shaking time of 30 min, solution pH of 4, room temperature, and activated charcoal amount of addition of 2.0 g/ L. Based on kinetic and thermodynamic studies, the sorption process for iron, fluoride, phosphate, COD and TSS on activated charcoal is said to follow pseudo-second order mechanism and exothermic nature.

Keywords: Sorption, wastewater, phosphate, fertilizer plant, and activated charcoal.

Correspondence to: M.S. Abdel Zaher, Abu Zaabal Fertilizer & Chemical Company, Tel: 01062380318 E-mail: msaad.phd2019@gmail.com

Received: January 25, 2020; **Accepted:** January 30, 2020; **Published:** February 28, 2020

Citation: Zeher M.S.A, Wahab S.M.A, Taha M.H (2021) Using activated charcoal for decrease iron, fluoride, phosphate, COD and TSS from wastewater of Phosphate Fertilizer plant. Pediatr Ther 11:219. doi: 10.35248/2329-891X.2021.11.219

INTRODUCTION

The Food and Agriculture Organization (FAO) defines food security as: "When all people, at all times, have physical, social and economic access to sufficient, safe and nutritious food that meets their dietary needs and food preferences for an active and healthy life" [1].

Population in the world is currently (2018-2019) growing at a rate of around 1.07% per year (down from 1.09% in 2018, 1.12% in 2017 and 1.14% in 2016). The current average population increase is estimated at 82 million people per year (Figure 1). The latest world population projections indicate that world population will reach 10 billion persons in the year 2055 and 11 billion in the year 2088 [2-3].

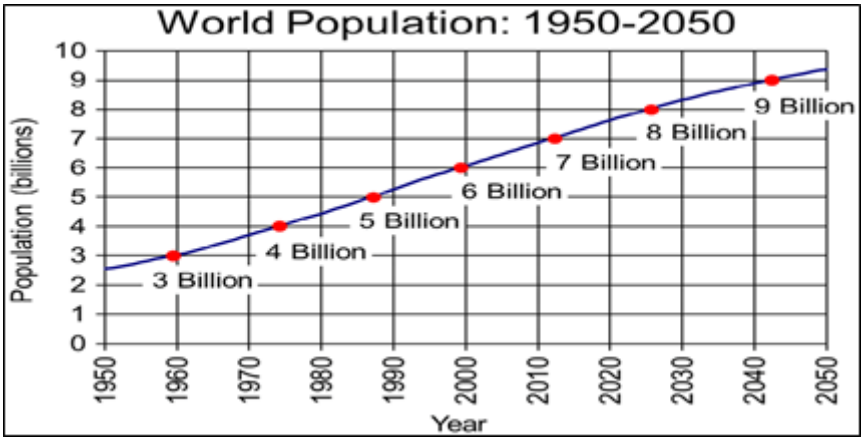

Figure 1: World population and projection from 1950- 2050; Dec. 2010 update

This increase in food production could be achieved by increasing agricultural output. Most of the increase is expected to come from producing more on existing farmland (i.e., intensification), although some new farmland will likely be needed [2].

The fertilizer industry is arguably one of the most important industries globally. Fertilizers provide food security and nutrition for the global population[4].

Phosphate fertilizers are produced by adding acid to ground or pulverized phosphate rock. If sulfuric acid is used, single or normal, phosphate (SSP) is produced, with a phosphorus content of16–21% P_2O_5. If phosphoric acid is used to acidulate the phosphate rock, triple phosphate (TSP) is the result. TSP has a phosphorus content of 43–48% as P_2O_5.The phosphate fertilizer plant used millions of gallons of water introducing phosphoric acid and

solid phosphate fertilizers. Phosphate fertilizer industries produce a particular kind of effluent which is highly acidic (pH=2) and contains significant amounts of pollutants such as: fluoride, phosphate, and other elements [5–7]. These pollutants are mainly present due to the use of rock phosphate. The high content in these pollutants and the enormous daily flow-rate of fertilizer industry wastewater from phosphoric acid and/or triple superphosphate (TSP) production lead to the discharge of several thousand tons of these elements per year [5, 6]. Thus, Wastewater treatment is a major problem in such complex fertilizer plant from the environmental pollution point of view.

Considering the growing environmental, economical, and technical concerns regarding fertilizer industry wastewater treatment, a variety of treatment strategies have been developed to reduce the contamination in pond water to facilitate reuse or discharge [8, 9]. Usually the industrial wastewater treatment employs one or more processes from physical, physico-chemical and biological methods. Conventional technologies for the removal of heavy metals such as chemical precipitation, ion exchange, electrolysis, and reverse osmosis are often neither effective nor economical. Among the physicochemical treatment, adsorption technique is cheap, effective, and easy to adapt [10].

Activated Carbons are the greatest influential adsorbents known. It is essentially a solid material involving mostly of pure carbon. A distinguishing feature is its porous structure and the resulting massive surface area which may be as great as 1500 m2/gm. Due to its excellent adsorption qualities, activated carbon is commonly used in process intended to disinfect, discolor, recover and eliminate odors at low cost and greater efficiency. Activated carbons effort on the principle of adsorption. Adsorption is an interfacial process including the collection of gaseous or solute constituents on the surface of adsorbent solids. This phenomenon is linked with physical attractive forces that bind gaseous and solute molecules typically known as Van-derWaals forces. Adsorption is thus a physical process, i.e. the constituents adsorbed on the surface do not feel any chemical reaction with the latter. The adsorbing solid is stated to as adsorbent and the substance to be adsorbed from the liquid or the gas phase as the solute. The adsorption influence and rate is determined by the generous of activated carbon, the particle size, the pore size and its distribution [11].

EXPERIMENTAL

Materials and Reagents

The used activated carbon (particle size 0.300–0.600 mm) was supplied by Jacobin Carbons Agents World Wide, Sweden. The activated carbon with high quality anthracite as raw material, its appearance is generally black granular activated carbon. The carbon sample was dried at 110 oC for 12 hrs. and then stored in dissector.

Collection of Wastewater Sample

Wastewater sample was obtained from Wastewater Lake; which used for collecting wastewater streams produced during fertilizer manufacture process in Abu Zaabal for Fertilizer and Chemicals Company (AZFC).The wastewater sample was preserved in refrigerator at 4°C for further use, therefore the potential for volatilization or

biodegradation of the sample can be minimized. The chemical analysis of the wastewater sample is given in Table (1) as analyzed in the central laboratory of AZFC Company.

Table (1): Chemical analysis of the wastewater working sample

Components	Concentration
pH	3.4
Turbidity (NTU)	150
Conductivity (µmho / cm)	10560
T.S.S (mg/L)	610
T.D.S (mg/L)	13200
COD (ppm)	290
Total hardness (ppm)	6500
P (ppm)	1120
SiO_2(ppm)	1751
SO_4 (ppm)	512
Cl^- (ppm)	205
F^- (ppm)	3400

Activated Charcoal Characterization

Mineral composition

The mineralogical analysis of activated charcoal sample has been carried out by using a powder X-ray diffract meter (model XD1180, Schimadzu, Japan) equipped with a copper target Cu Kα radiation under target voltage 40 KV and current 30 mA in (a scanning rate of 2o/ min).

Chemical composition

The elemental analyses of activated charcoal sample have been performed by X-ray fluorescence (XRF) using Philips PW-2400 sequential X-ray spectrometer (Japan).

Fourier transform infrared (FTIR) spectrum

The identification of the surface functional groups of activated charcoal sample were carried out in the mid-infrared region from 4000 to 500 cm−1with PerkinElmer Spectrum BX Infrared spectrometer under ambient air condition using KBr as diluent.

Surface area

The specific surface area of activated charcoal sample was measured by BET method using Nova 2000 quantachrome. The moisture and gases on the solid surface or the penetrated in the open pores were removed by heating at 120°C for 2h prior to the surface area measurements.

Apparatus

The reaction was carried out in a cylindrical 250 ml reactor of 10 cm diameter. It was fitted with Teflon-coated stirrer with 2 cm diameter and placed in thermostatically controlled water bath. The impeller tip speed was adjusted at 300 rpm. Filtration was performed using Buchner type filter of 4.6 inch, Diameter. Polypropylene filter cloth of 80 mesh aperture size was used. A vacuum pump was used for filtration.

Experimental Procedures

Unless otherwise stated, Batch adsorption experiments were performed by shaking 2.0 g of activated charcoal with1000 mL of the wastewater in a thermo stated shaker bath at (25 ± 1oC). After the corresponding time interval, the solutions were filtered through a 0.45 μm pore size membrane. Iron and phosphate ions concentration in the filtrate was determined using an inductively coupled plasma optical emission spectrometer (Optima 2100DV, Perkin-Elmer).Fluoride concentration in the filtrate was measured by a Fluoride ion selective electrode (Thermo Scientific Orion Star A215 pH/ Conductivity Bench top Meter (USA) coupled to an 8157BNUMD Orion ROSS Ultra Triode pH/ATC electrode). Chemical oxygen demand (COD) was measured by titrimetric method and Total suspended solids (TSS) were measured by gravimetric method.

The sorption capacity (qe, mg/g) was calculated using the following equation:

$$q_e = (C_o - C_e) \times \frac{V}{m} \text{.....(1)}$$

Where Co and Ce are the initial and equilibrium concentrations of iron, fluoride, and phosphate ions (mg/L), respectively, V is the volume of the wastewater (L), and m is the weight of activated carbon used (g). The removal efficiency (R) of Fe, P, F ions from working waste solution was calculated as follows:

$$R\ \% = \frac{C_o - C_e}{C_o} \times 100 \text{.....(2)}$$

The distribution coefficient (Kd) of iron, fluoride, and phosphate ions between the aqueous bulk phase and the solid phase was calculated through the following equation:

$$K_d = \frac{C_o - C_e}{C_o} \times \frac{V}{m} \text{.....(3)}$$

COD Content has been measured according to the following relation [12].

COD (mg/L) = (A-B) x M x (8000/V)

Where: A and B are the volume of FAS utilized for blank and sample respectively, M is the molarity of FAS (ferrous ammonium sulfate).

The total suspended solids has been measured according to the following relation [13]

TSS (mg/L) = (A-B)/V

Where: A is the mass of filter + dried residue (mg), B is the mass of filter (mg), and V is the filtered sample volume (L).

RESULTS AND DISCUSSION

Characterization of the Activated Charcoal

Texture Characteristics

The surface properties and morphological characteristics of the applied activated carbon have been discussed through Table 2 and Figures 2.

Table 2: Surface characteristics of blank and metals functionalized bio-char.

Physical properties	Activated carbon
BET surface area (m^2/g)	1171
Average pore radius (nm)	1.9
Total pore volume (cm^3/g)	0.55
Micro porosity (vol. %)	69

According to the presented data in Table 2, it is clear that the applied activated carbon structure showed elevated specific surface area value (1171m2/ g). This has been further confirmed through the given total pore volume (0.55 cm3/ g). These values indicate that the applied carbon sorbent has large surface area, and hence more available active sites.

The inner morphology of activated carbon working sample has been illustrated in Figures 2.

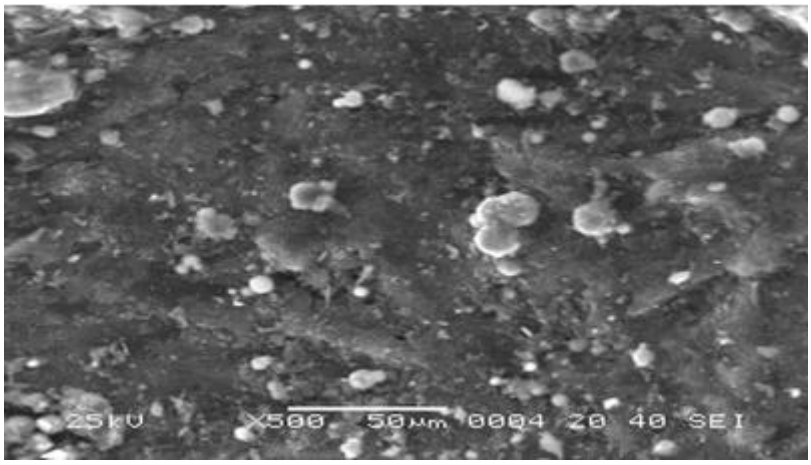

Figure 2: Inner morphological characteristics of activated charcoal.

In reference to Figure 2, it is indicated that the activated carbon sample had exhibited loose aggregates with a porous structure. Moreover, it is clear that the carbon surface is smooth and distributed with small pores which confirm the data obtained in Table 2. The Figure also show some salt particles which are scattered on the surface of activated carbon due to the remaining some metal compounds on the carbon surface [14].

Structural Properties

The structural characteristics of the applied activated carbon particles had been illustrated through the displayed XRD and Ft-IR spectrums in Figures 3-3.17.

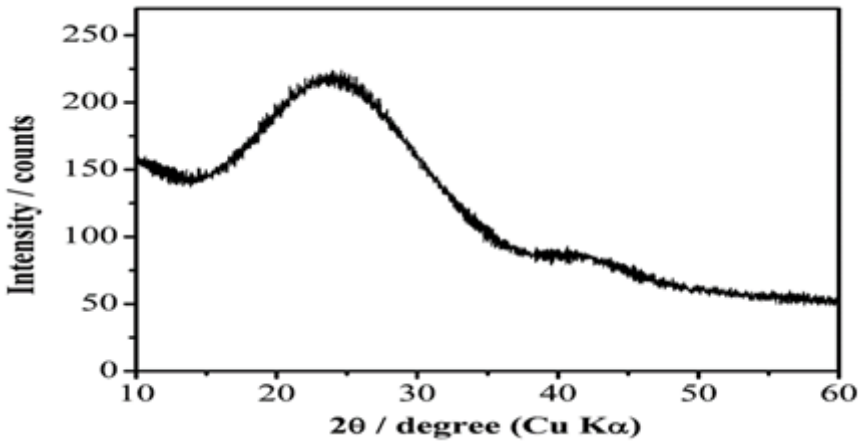

Figure 3 : XRD patterns of activated carbon sorbent.

XRD spectrum in Figure 3 illustrates the presence of intense broad peak located between 2θ of 20o and 30o which is the main indicative peak for the presence of a carbonaceous structure. Additional peak referring to the charcoal can be noticed between 2θ of 40o. The observed broad peaks are generally reflecting the amorphous nature of the presented structure.

Nevertheless, low intense sharp peaks could be detected alongside the whole of the exhibited XRD spectrum. This may indicate the presence of some incorporated crystalline structures within the amorphous particles of bio-char. The increased intensity of the indicative peaks for amorphous structure than those of the crystalline ones refers to the domination of amorphous nature in the introduced structure. Although the XRD signals exhibit amorphous nature of the produced bio-carbon, it presented a high surface area, as prior cleared. The results showed that SiO2 has the highest percentage of all the compound and element present as revealed by the XRD analysis. Complete

Mineralogical analysis carried out by X-ray diffraction also revealed that the activated charcoal contains each of these elements C, O, Mg, Al, Si" Fe, Na, K, Zn. The XRD result showed that both SiO2 and SiC have a fine structure, the former having a finer one. This could be associated with pore size [15].

The structural characteristics of the revealed carbon structure through this research study had been further illustrated via FT-IR spectra. This type of analysis was used to discover varieties of existing function groups in the prepared bio-char and its metals oxides functionalized structures. FTIR technique is a useful analytical method which can provide sharp tracking for the changes in the structure through the increase and decreases in the intensity of the detected peaks. It can also show occurring influence on certain structures due to the different operating conditions. The FT-IR spectroscopic study of the utilized activated carbon is presented in Figure 4.

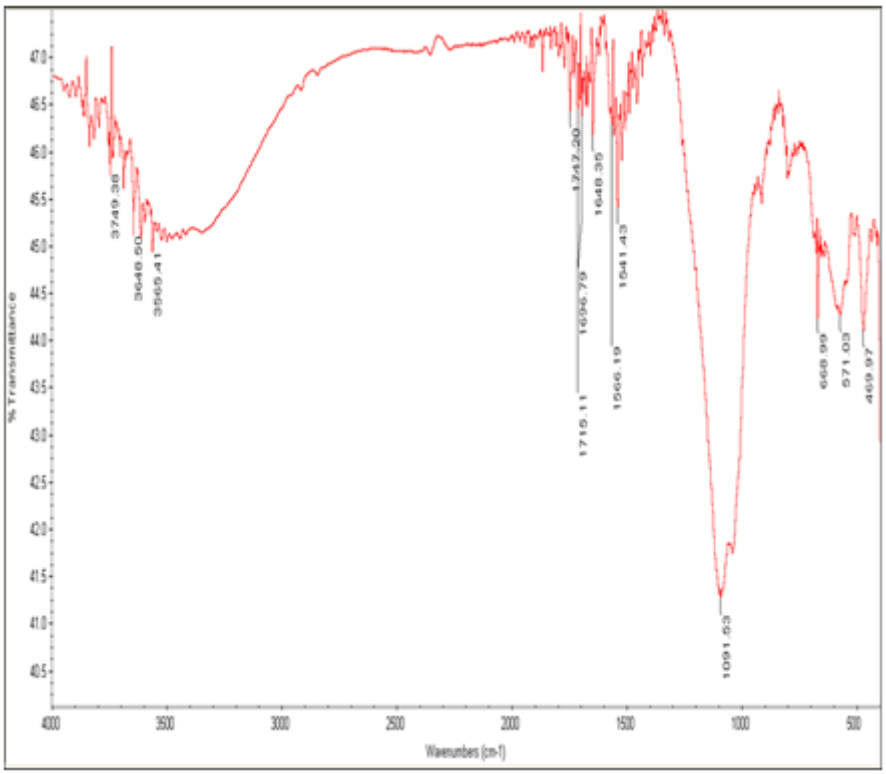

Figure 4 : FT-IR spectrums of activated carbon species.

The presented FTIR spectra in Figure 4 showed three major absorption bands at around 3400-3740 cm-1, 1100- 1750 cm-1 and 400-850 cm-1 however the acid sites functionalized activated carbon showed additional bands than that of the blank carbon. In the first region of absorption, a wide band with a reasonable intensity can be noticed at 3400 cm-1 in both structures. This band is due to O-H stretching mode of both the hydroxyl groups and adsorbed water which might exist in the two structures. In addition, it must be indicated that the bands in the range of 3200-3750 cm-1 have also been referred to the occurring hydrogen bonding between the OH groups [16].

For the second major absorption, the noted peak at 1640 cm-1 is indicative to the amides that can be distinguished on the surface of the activated carbons. The presence of such functional group could be obtained during the activation process owing to the presence of primary amines that in the biomass based feedstock. The peak at approximately 1150 cm-1 belongs to the fingerprint of this carbon. This band can also be associated with C-O symmetric and asymmetric stretching vibration of -C-O-C- ring [17].

The third region show peak at 628 cm-1 is assigned to the C-H bending mode. Moreover, the region in between 700 - 900 cm-1 contains various bands related to C-H bending with different degrees of substitution [18]. The bending region for the activated carbon might indicate that the existing aliphatic C-H. This in turn can clarify that most of the aliphatic structures in the activated carbon are cyclic structures.

XRF Study

The chemical composition of the applied activated charcoal particles had been illustrated through the X-ray fluorescence (XRF) analysis is represented in Table 3.

Table 3: XRF analysis of activated charcoal

Element	SiO_2	Al_2O_3	CaO	Fe_2O_3	K_2O	MgO	Na_2O	MnO	ZnO
%	45.05	15.6	0.57	12.4	0.52	16.2	0.45	0.22	0.3

XRF analysis confirmed that SiO2, Al2O3, MgO and Fe2O3 were found to be major constituents of the ash. Silicon dioxide, iron oxide and alumina are known to be among the hardest substances. Some other oxides viz. CaO, K2O, Na2O and MnO were also found to be present in traces. The presence of hard elements like SiO2, Al2O3 and Fe2O3 suggested that, the activated charcoal can be used as particulate reinforcement in various metal matrixes. This result of XRF is in agreement with the result of XRD obtained and FT-IR analysis [19].

Batch investigation

In this section, the impact of numerous variables on the adsorption behavior of the activated charcoal has been studied, by batch technique, to figure out the optimal adsorption conditions that could achieve effective removal of iron, fluoride, phosphate, and COD and TSS from wastewater sample. These parameters include mixing time (2- 120 min), sorption temperature (25- 65±1 oC), solution pH (1-10), mechanical stirring speed (25- 150 rpm), and sorbent amount of addition (0.25 – 3 g/ L).

Effect of Shaking Time

The effect of contact time on iron, fluoride, phosphate, and COD and TSS from wastewater onto activated charcoal sorbents was investigated at shaking time ranging from 2 to 120 min. The other factors were sorbent dose; 2 g/ L, solution pH of 4, mechanical stirring speed of 100 rpm, and reaction temperature of 25±1oC. The results of iron, fluoride, phosphate, COD and TSS adsorption kinetics are shown in Tables 4 and 5 , and presented in Figure 5 as a relation between sorption efficiency and time. From the Figure it is indicated that, the rate of iron, fluoride, phosphate, COD and TSS uptake increased rapidly for the applied sorbent and reached 34.2, 75.9, 80.4, 81.4, and 87.7% respectively at initial time of 30 min (stage I). Further increase in contact time up to 120 min brings no significant increase in Fe, F, P, COD and TSS removal percentage (stage II). This behavior could be due to the availability of adsorbent active groups and reaction sites (Stage I) [20-21].

The adsorption rate of Fe, F, P, and COD and TSS species were slow in stage II due to they occupied most of the sorbents active sites, and thereby further adsorption needed longer time to bond with the inside active sites which affecting the adsorption rate [22]. These results suggested that Fe, F, P, COD and TSS sorption process was dominated by surface sorption and intraparticle diffusion for the utilized activated charcoal [23]. Therefore, other sorption experiments were conducted at 30 min.

Time (min)	Fe		F		P	
	Concentration (ppm)	Sorption E (%)	Concentration (ppm)	Sorption E (%)	Concentration (ppm)	Sorption E (%)
2	286	7.7	3070	9.7	1000	10.7
5	276	11	2610	23.2	890	20.5

10	250	19.4	1920	43.5	650	42
20	232	25.2	1410	58.5	450	59.8
30	204	34.2	820	75.9	220	80.4
60	200	35.5	785	76.9	216	80.7
120	195	37.1	772	77.3	176	84.3

Table 4: Effect of time on Fe, F, and P sorption efficiency, % (solution pH is 4; 2 g sorbent/L of wastewater; temperature 25 ± 1°C, 100 rpm).

Table 5 : Effect of time on COD, and TSS sorption efficiency, % (solution pH is 4; 2 g sorbent/L of wastewater; temperature 25 ± 1°C, 100 rpm).

Time (min)	COD		TSS	
	Concentration (ppm)	Sorption E (%)	Concentration (ppm)	Sorption E (%)
2	240	17.2	520	14.8
5	210	27.6	460	24.6
10	172	40.7	340	44.3
20	122	57.9	162	73.4
30	54	81.4	75	87.7
60	50	82.8	64	89.5
120	46	84.1	56	90.8

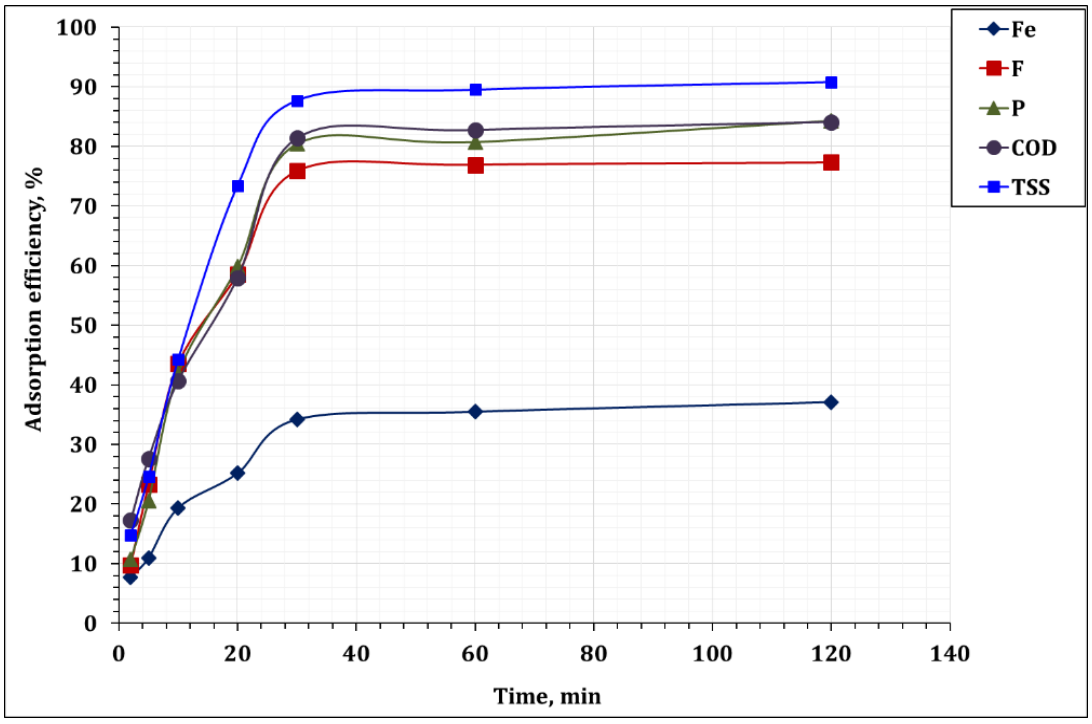

Figure 5 : Effect of time on Fe, F, P, COD and TSS sorption efficiency, % (solution pH is 4; 2.0 g sorbent/L of wastewater; temperature 25 ± 1°C, 100 rpm).

Effect of the Temperature

To study the effect of temperature on iron, fluoride, phosphate, COD and TSS adsorption from wastewater using activated charcoal, a set of experiments have been investigated within the range of 25– 65 ±1oC at amount of addition 2 g/ L, reaction time of 30 min, solution pH is 4, and stirring speed of 100 rpm. The collected experimental results are presented in Tables 6 and 7 and graphically plotted in Figure 6 as a relation between sorption efficiency and reaction temperature.

The obtained results revealed that the temperature variation from 25 to 65 oC had negative impact on iron, fluoride, phosphate, COD and TSS sorption efficiency. Numerically, the increase of temperature from 25 to 65 oC, decrease iron, fluoride, phosphate, COD and TSS sorption efficiency from 34.2 to 23.5 %, from 75.9 to 72.2%, from 80.6 to 75.4%, from 81.7 to 60.3, and from 87.9 to 82.8% respectively. This behavior indicates that iron; fluoride, phosphate, COD and TSS adsorption from wastewater using the presented carbon structure is an exothermic reaction.

Table 6 : Effect of temperature on Fe, F and P sorption efficiency, (time 30 min; sorbent dosage 2.0 g/L; 100 rpm; pH 4).

Temperature (°C)	Fe		F		P	
	Concentration (ppm)	Sorption E (%)	Concentration (ppm)	Sorption E (%)	Concentration (ppm)	Sorption E (%)
25	204	34.2	820	75.9	217	80.6
35	209	32.6	835	75.4	225	79.9
45	218	29.7	890	73.8	241	78.5
55	228	26.5	915	73.1	259	76.9
65	237	23.5	944	72.2	276	75.4

Table 7 : Effect of temperature on COD and TSS sorption efficiency, (time 30 min; sorbent dosage 2.0 g/ L; 100 rpm; pH 4).

Temperature (°C)	COD		TSS	
	Concentration (ppm)	Sorption E (%)	Concentration (ppm)	Sorption E (%)
25	53	81.7	74	87.9
35	62	78.6	78	87.2
45	81	72.1	87	85.7
55	98	66.2	97	84.1
65	115	60.3	105	82.8

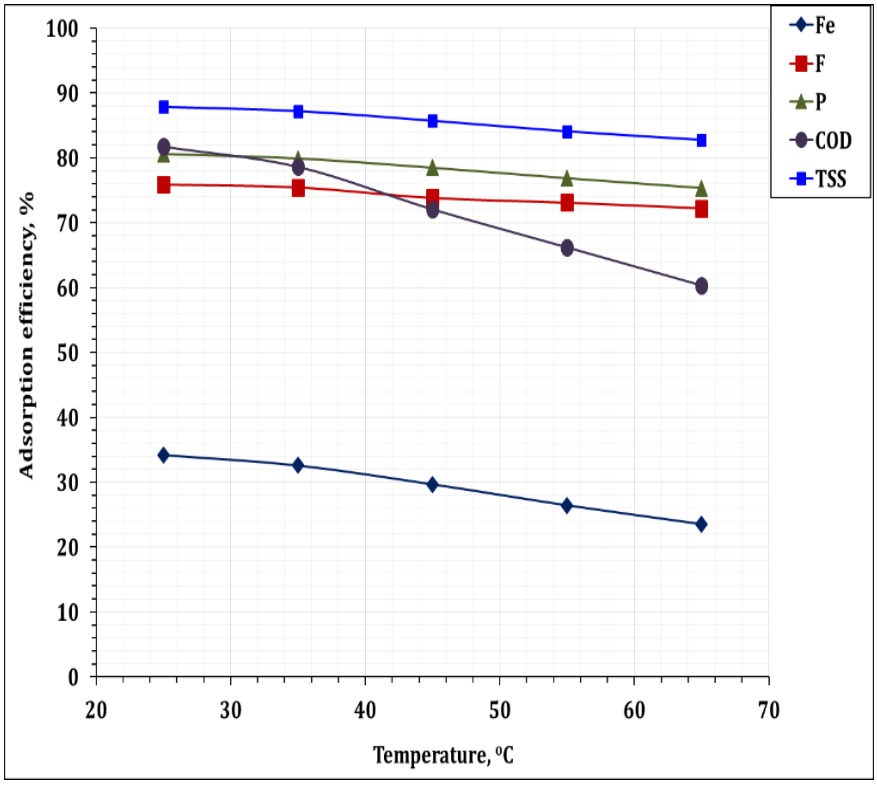

Figure 6 : Influence of temperature on Fe, F, P, COD and TSS adsorption efficiency, % (reaction time 30 min; 100 rpm; pH 4; sorbent dosage 2.0 g/L).

Effect of solution pH

It is well known that, pH values display a significant impact on adsorption [24]. The initial pH of the adsorbate solution influences the adsorption process by changing the adsorbent's functional group [25]. In this regards, the effect of solution pH ranging from 1-5 on the Fe, P, F ions TSS and COD And sorption using activated charcoal from wastewater has been investigated by shaking 2.0 g of the sorbent with 1.0 L wastewater for 30 min at temperature of 25 ± 1oC and stirring speed of 100 rpm. The experimental results are shown in Tables 8 and 9 and presented through Figure 7 as a relation between adsorption efficiency and solution pH.

The Figure show that, by increasing the solution pH from 1 to 4, the adsorption % remarkably increased from 9.0 to 34.1% for iron, from 16.2 to 75.8 % for fluoride, from26.3 to 80.4 for phosphate, from 21.4 to 81.4 for COD, and from 32.8 to 87.7 for TSS. This may be attributed to the increase of positive charge on the activated carbon surface. Further increase in solution pH up to 10 has dramatically negative effect on iron, fluoride, phosphate, COD, and TSS sorption efficiency. This behavior may be due to the decrease of the positive charge and increase of the negative charge on the charcoal active surface increase of the positive charges on activated carbon surface. The negatively charged AC surface does not favor the adsorption of anion due to the electrostatic repulsion [26]. Thus, pH of 4 was selected for further sorption studies.

Table 8 : Effect of solution pH on Fe, F, and P sorption efficiency, % (sorbent dosage 2.0 g/ L; shaking time 30 min; room temperature; 100 rpm).

Solution pH	Fe		F		P	
	Concentration (ppm)	Sorption E (%)	Concentration (ppm)	Sorption E (%)	Concentration (ppm)	Sorption E (%)
1	282	9	2850	16.2	825	26.3
2	264	14.8	2530	25.6	554	50.5
3	248	20	1720	49.4	576	48.6
4	204	34.1	823	75.8	220	80.4
5	224	27.8	1198	64.8	380	66.1
8	249	19.8	1686	50.4	648	42.1
10	275	11.2	2298	32.4	799	28.7

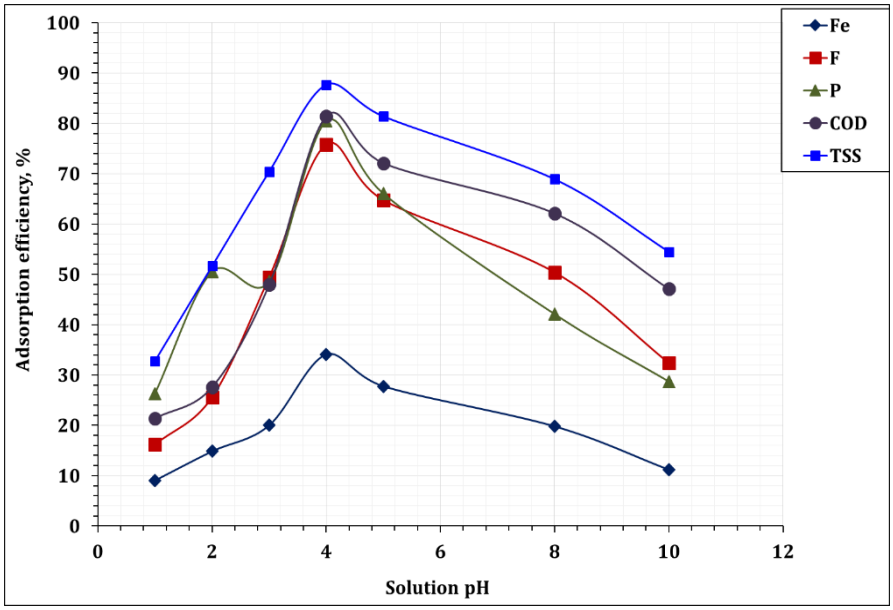

Figure 7 : Effect of solution pH Fe, F, P, COD and TSS sorption efficiency, % (sorbent dosage 2.0 g/ L; shaking time 30 min; room temperature; 100 rpm).

Effect of Mechanical stirring speed:

To investigate the effect of stirring speed on iron, fluoride, phosphate, and COD and TSS recovery from wastewater, several experiments have been carried out at room temperature, sorbent dosage, 2.0 g/ L, and time of 30 min; however the stirring speed was ranged from 25 to 150 rpm. The results of Fe, F, P, COD and TSS sorption % versus the increase of mechanical stirring speed are presented in Tables 10 and 11 and plotted in Figure 8.

From the Figure, it is clear that by increasing the stirring speed from 25 to 100 rpm, iron adsorption efficiency improved from 11.6 to 34.2%, fluoride sorption percent enhanced from 34.4 to 75.9%, phosphate adsorption increased from 29.5 to 80.4%, COD improved from 34.5 to 81.4%, and finally TSS adsorption enhanced from 46.7 to 87.7%. Thus the mechanical stirring speed has remarkably effect on Fe, F, P, COD and TSS adsorption onto introduced carbon based adsorbent. Therefore, 100 rpm was the chosen stirring rate.

Table 10 : Effect of stirring speed on Fe, F, and P sorption efficiency, % (Shaking time 30 min; sorbent dosage 2.0 g/L; room temperature; solution pH is 4).

Stirring speed (rpm)	Fe		F		P	
	Concentration (ppm)	Sorption E (%)	Concentration (ppm)	Sorption E (%)	Concentration (ppm)	Sorption E (%)
25	274	11.6	2230	34.4	790	29.5
45	248	20	1792	47.3	610	45.5
65	230	25.8	1357	60.1	390	65.2
85	217	30	1057	68.9	285	74.6
100	204	34.2	820	75.9	220	80.4
150	198	36.1	780	77.1	220	80.4

Table 11 : Effect of stirring speed on COD and TSS sorption efficiency, % (Shaking time 30 min; sorbent dosage 2.0 g/L; room temperature; solution pH is 4).

Stirring speed (rpm)	COD		TSS	
	Concentration (ppm)	Sorption E (%)	Concentration (ppm)	Sorption E (%)
25	190	34.5	325	46.7
45	123	57.6	243	60.2
65	80	72.4	135	77.9
85	68	76.6	118	80.7
100	54	81.4	75	87.7
150	50	82.8	60	90.2

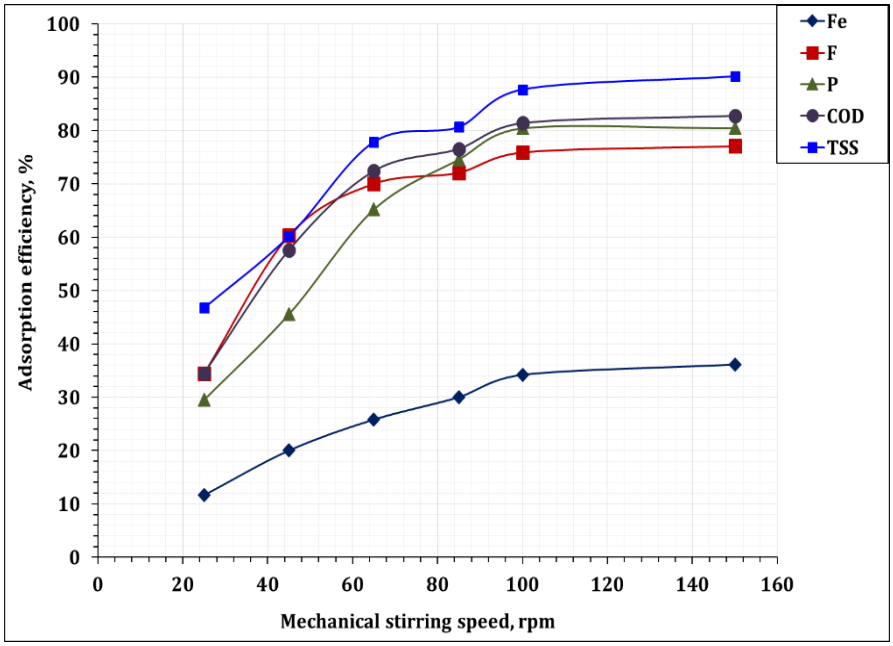

Figure 8: Effect of stirring speed on Fe, F, P, COD and TSS adsorption efficiency, % (reaction time 30 min; sorbent dose 2.0 g/L; room temperature; pH is 4).

Effect of adsorbent amount

To explore the optimum adsorbents amount of addition, the effect of sorbents amount of addition, ranging from 0.25 to 3.0 g/ L on the sorption efficiency of iron, fluoride, phosphate, and COD and TSS from wastewater, onto activated charcoal was studied. The operating conditions used were, room temperature, reaction time of 30 min, and stirring speed of 100 rpm. The obtained results are exhibited in Tables 12 and 13 and illustrated in Figure 9 as a relation between adsorption efficiency % and sorbent amount of addition. The results show that the increase of sorbent amount of addition from 0.25 to 2.0g/ L enhanced the adsorption ability of activated charcoal for Fe, F, P, COD and TSS.

Numerically, as the sorbent amount of addition increased from 0.25 – 2.0g/ L, the Fe, F, P, COD and TSS adsorption efficiency raises from 12.9 to 34.2%, 26.8 to 75.9%, 21.4 to 80.4%, 37.9 to 81.4%, and 52.5 to 87.7% respectively. This indicating that Fe, F, P, COD and TSS sorption into activated charcoal adsorbent was strongly affected by the solid content ranging from 0.25 to 2.0g/ L. This behavior could be due to presence of more active sites as well as more high-activity particles [27]. Further increase of the sorbent dose up to 3.0g/ L (high solid content), has slightly effect on the sorption process, this may be attributed to the adsorption reaction of Fe, F, P, COD and TSS reached equilibrium and produced high solid accumulation effect [28]. Accordingly, the solid/ liquid ratio, 2.0g/ L was the chosen ration during all the other experiments.

Interestingly, qe values for Fe, F, P, COD and TSS adsorption decreased from 160 to 40.4 mg/g for iron, from 3640 to 894 mg/ g for fluoride, from 960 to 314 mg/g for phosphate, from 440 to 82.4 mg/ g for COD, and from 1280 to 190 mg/ g for TSS with the solid content increasing from 0.25 to 3.0 mg/L Figure 10 . This behavior could be attributed to there is no free available sites on adsorbate for reacting with Fe, F, P, COD and TSS [27-28].

Table 12 : Effect of solid/ liquid ratio on Fe, F, and P adsorption % (reaction time 30 min; 100 rpm; room temperature; pH of 4).

Dosage (g/L)	Fe		F		P	
	Concentration (ppm)	Sorption E (%)	Concentration (ppm)	Sorption E (%)	Concentration (ppm)	Sorption E (%)
0.25	270	12.9	2490	26.8	880	21.4
0.5	253	18.4	1838	45.9	642	42.7
1	225	27.4	1230	63.8	310	72.3
2	204	34.2	820	75.9	220	80.4
2.5	192	38.1	762	77.6	195	82.6
3	189	39.1	717	78.9	178	84.1

Table 13 : Effect of solid/ liquid ratio on COD and TSS adsorption % (reaction time 30 min; 100 rpm; room temperature; pH of 4).

Sorbent dosage (g/ L)	COD		TSS	
	Concentration (ppm)	Sorption E (%)	Concentration (ppm)	Sorption E (%)
0.25	180	37.9	290	52.5
0.5	136	53.1	215	64.8
1	92	68.3	145	76.2
2	54	81.4	75	87.7
2.5	47	83.7	47	92.3
3	43	85.2	41	93.3

Table 14 : Effect of solid/ liquid ratio on Fe, F, P, COD, and TSS adsorption capacity, qe (mg/ g).

Dosage (g/ L)	Fe	F	P	COD	TSS
	Qe (mg/ g)				
0.25	160	3640	960	440	1280
0.5	114	3124	956	308	790
1	85	2170	809.8	198.1	465
2	53	1292	451.9	117.7	265.7
2.5	47	1055.4	370	97.1	225.2
3	40	894.2	314	82.4	189.7

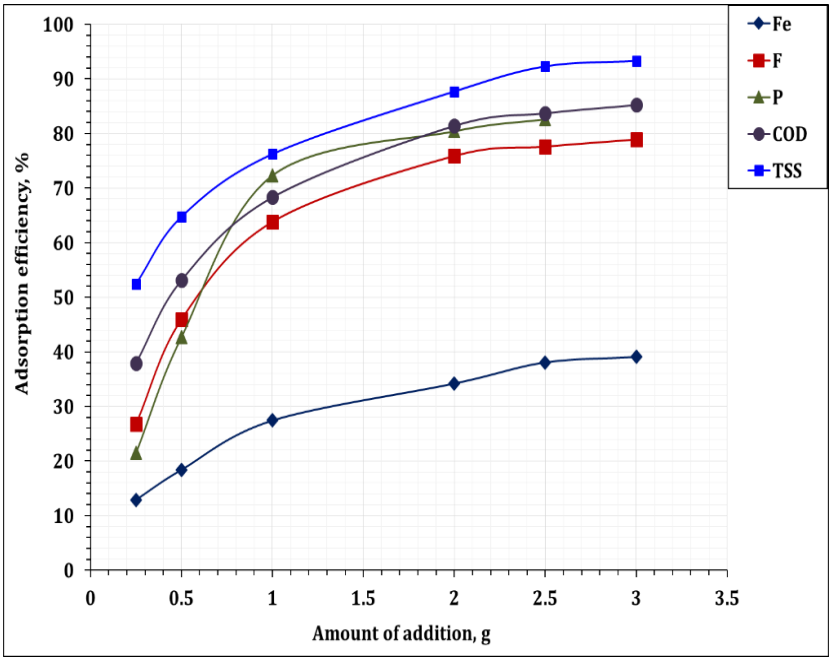

Figure 9 : Effect of solid/ liquid ratio on Fe, F, P, COD and TSS adsorption % (reaction time 30 min; 100 rpm; room temperature; pH of 4).

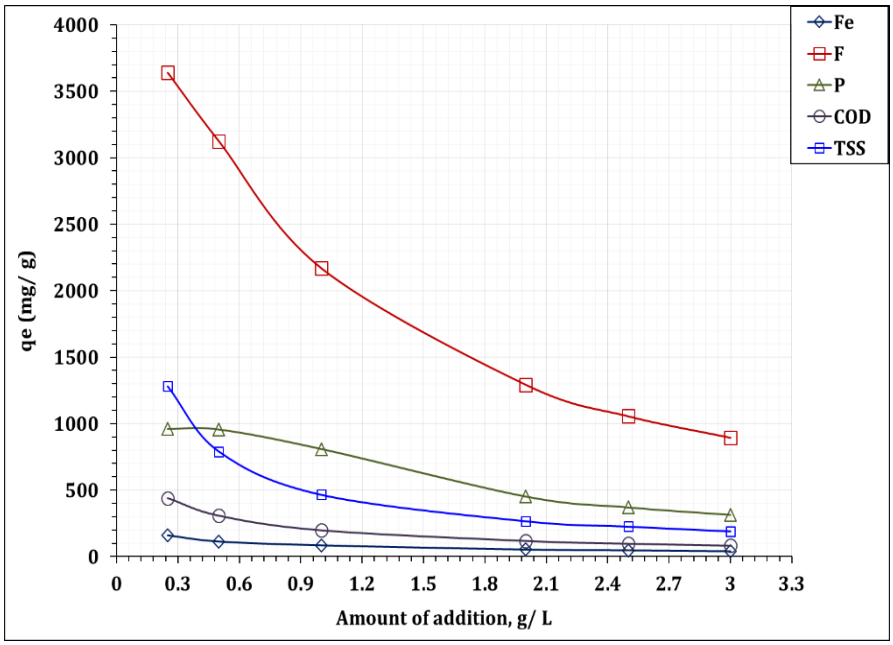

Figure 10 : Effect of solid/ liquid ratio on Fe, F, P, COD, and TSS adsorption capacity, qe (mg/ g).

Sorption Kinetic Modeling

Kinetic studies reveal valuable information such as the iron, fluoride, phosphate, and COD and TSS adsorption mechanism and the solute maximum uptake rate which are necessary to design the column parameters in the recovery process. In this respect, pseudo- first- order model, pseudo- second- order model (as an example for adsorption reaction models), and Weber- Morris model, (as an example for adsorption diffusion model) were

applied to interpret the experimental results of Fe, F, P, COD and TSS adsorption from wastewater stream sample onto activated charcoal at 25±1 °C.

The adsorption models; Lagergreen pseudo first-order model, pseudo second kinetic model and Weber- Morris model have been described in section 3.1.3. To figure out the kinetics of iron, fluoride, phosphate, and COD and TSS sorption process, the experimental data obtained in Tables 12-13 and 14 were used to calculate the difference model functions; (q_t), (t/ q_t), and ($\log (q_e - q_t)$), as shown in Tables (15-16-17-18-19) for iron, fluoride, phosphate, COD and TSS sorption respectively.

Table 15: The values of (q_t), ($\log (q_e - q_t)$), and (t/q_t) for iron sorption using activated charcoal relative to shaking time.

Time (min)	$t^{1/2}$	Ce	q_t	$\log (q_e-q_t)$	t/q_t
2	1.4	286	24	1.96	0.083
5	2.2	276	34	1.91	0.147
10	3.2	250	60	1.74	0.167
20	4.5	232	78	1.57	0.256
30	5.5	204	106	0.95	0.283
60	7.7	200	110	0.7	0.545
120	11	195	115	*	1.043

Table 16: The values of (q_t), ($\log (q_e - q_t)$), and (t/q_t) for fluoride sorption using activated charcoal relative to shaking time.

Time (min)	$t^{1/2}$	Ce	q_t	$\log (q_e-q_t)$	t/q_t
2	1.4	3070	330	3.36	0.006
5	2.2	2610	790	3.26	0.006
10	3.2	1920	1480	3.06	0.007
20	4.5	1410	1990	2.8	0.01
30	5.5	820	2580	1.68	0.012
60	7.7	785	2615	1.12	0.023
120	11	771.8	2628.2	*	0.046

Table 17: The values of (q_t), ($\log (q_e - q_t)$), and (t/q_t) for phosphate sorption using activated charcoal relative to shaking time.

Time (min)	$t^{1/2}$	Ce	q_t	log (q_e-q_t)	t/q_t
2	1.4	1000	120	2.92	0.017
5	2.2	890	230	2.85	0.022
10	3.2	650	470	2.68	0.021
20	4.5	450	670	2.44	0.03
30	5.5	220	900.5	1.64	0.033
60	7.7	216	904	1.6	0.066
120	11	176	944.2	*	0.127

Table 18: The values of (qt), (log (qe − qt)), and (t/qt) for COD sorption using activated charcoal relative to shaking time.

Time (min)	$t^{1/2}$	Ce	q_t	log (q_e-q_t)	t/q_t
2	1.4	240	50	2.29	0.04
5	2.2	210	80	2.21	0.063
10	3.2	172	118	2.1	0.085
20	4.5	122	168	1.88	0.119
30	5.5	54	236	0.9	0.127
60	7.7	50	240	0.59	0.25
120	11	46	243.89	*	0.492

Table 19: The values of (qt), (log (qe − qt)), and (t/qt) for TSS sorption using activated charcoal relative to shaking time.

Time, min	$t^{1/2}$	Ce	q_t	log (q_e-q_t)	t/q_t
2	1.4	520	90	2.67	0.022
5	2.2	460	150	2.61	0.033
10	3.2	340	270	2.45	0.037
20	4.5	162	448	2.02	0.045
30	5.5	75	535	1.28	0.056
60	7.7	64	546	0.9	0.11
120	11	56	553.88	*	0.217

The scatter plot of log (qe - qt) versus time for Lagergreen pseudo first-order model (Figure 11), the plot of (t/qt) versus time for pseudo second kinetic model (Figure 12), and the plot of qt versus t0.5 for Morris-Weber model (Figure 13), have been illustrated and used for evaluating the kinetic constants for iron, fluoride, phosphate, and COD and TSS sorption process using activated charcoal. The correlation coefficients (R^2) value and the values of kinetic constants have been tabulated in Table 20-21.

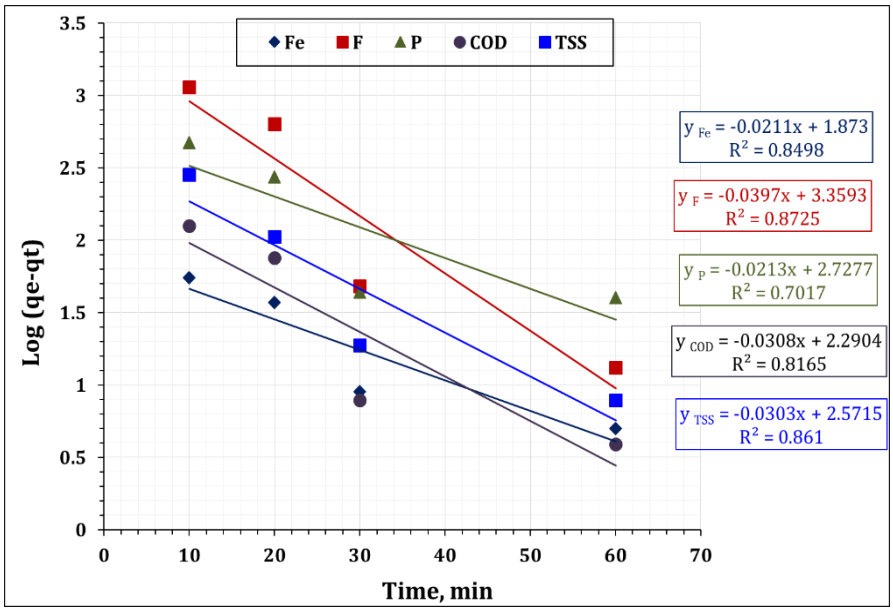

Figure 11 : Lagergreen plot for iron, fluoride, phosphate, and COD and TSS adsorption from wastewater using activated charcoal.

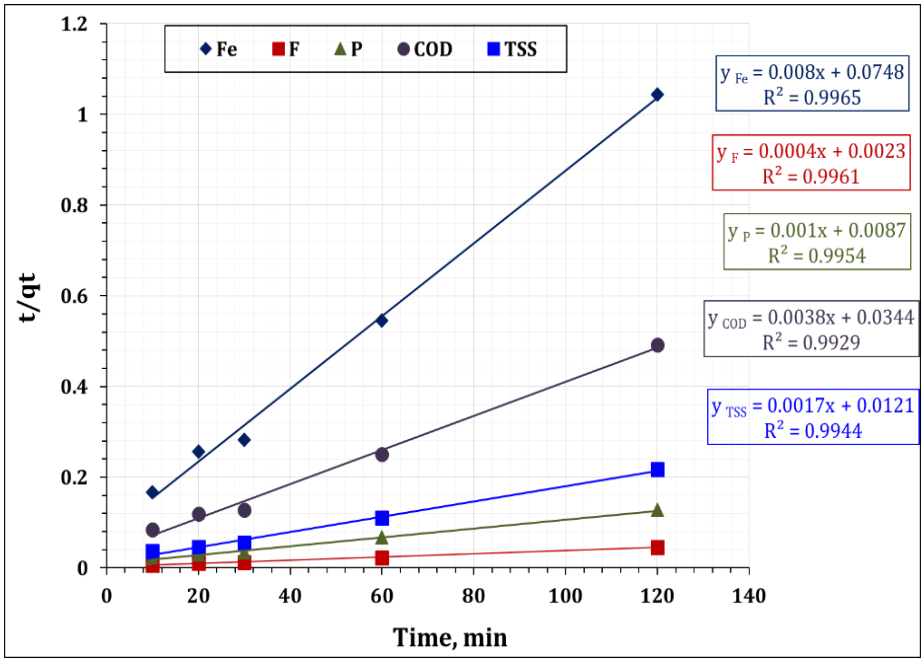

Figure 12 : Pseudo second-order plot for iron, fluoride, phosphate, and COD and TSS adsorption from wastewater using activated charcoal.

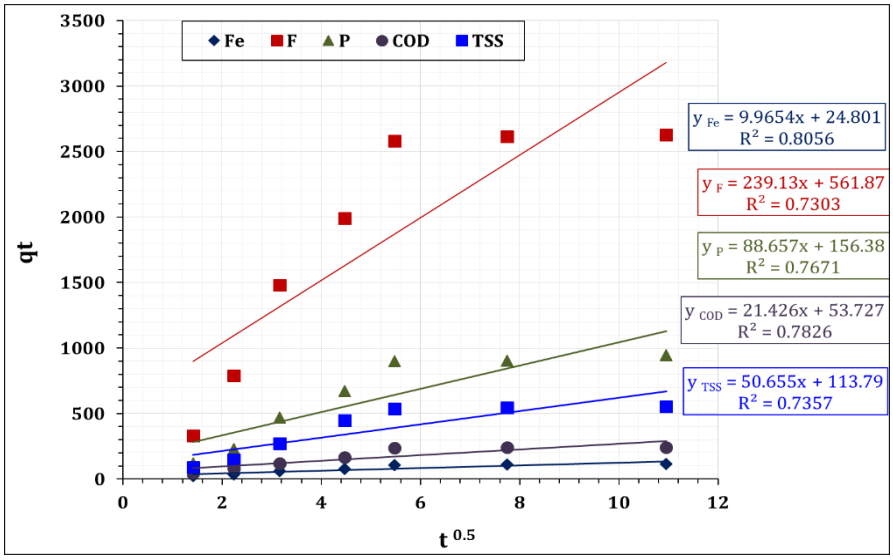

Figure 13 : Morris-Weber plots for iron, fluoride, phosphate, and COD and TSS adsorption from wastewater using activated charcoal.

Table 20 : The calculated parameters of pseudo first-order, pseudo second-order, and Morris-Weber kinetic models for iron, fluoride, and phosphate.

		Fe	F	P
Lagergreen pseudo first-order	K_1 (min $^{-1}$)	0.05	0.09	0.05
	qe_{cal} (mg/ g)	75	2287	534
	qe_{exp} (mg/ g)	115	2628	944
	R^2	0.85	0.87	0.71
Pseudo second-order	K_2 (min $^{-1}$)	0.0009	0.0001	0.0001
	$q_{e\ cal}$ (mg/ g)	125	2500	1000
	$q_{e\ exp}$ (mg/ g)	115	2628	944
	R^2	0.99	0.99	0.99
Weber and Morris model	K_i (mg/g min$^{1/2}$)	10	239.1	88.7
	C	24.8	561.9	156.4
	R^2	0.8	0.73	0.76

Table 21: The calculated parameters of pseudo first-order, pseudo second-order, and Morris-Weber kinetic models for COD and TSS.

		COD	TSS
Lagergreen pseudo first-order	K_1 (min^{-1})	0.07	0.07
	$q_{e\ cal}$ (mg/ g)	195	373
	$q_{e\ exp}$ (mg/ g)	244	554
	R^2	0.81	0.86
Pseudo second-order	K_2 (min^{-1})	0.0004	0.0002
	$q_{e\ cal}$ (mg/ g)	263	588
	$q_{e\ exp}$ (mg/ g)	244	554
	R^2	0.99	0.99
Weber and Morris model	K_i (mg/g $min^{1/2}$)	21.4	50.7
	C	53.7	113.8
	R^2	0.78	0.73

Analysis of the kinetic models was employed to investigate the adsorption rate and uptake mechanism of iron, fluoride, phosphate, and COD and TSS species sorption onto activated charcoal. In the present experimental data, the suitability of the kinetic models was measured using correlation coefficient (R2) values and comparison between experimental and calculated value of adsorption capacity.

From the results shown in Table 20 - 21, it can be seen that the calculated qe values from pseudo-second-order agree very well with the experimental qe values. In addition, the correlation coefficients for iron, fluoride, phosphate, COD and TSS adsorption are ≥0.99. Therefore, the adsorption kinetics of iron, fluoride, phosphate, COD and TSS from wastewater onto activated charcoal are described by pseudo second-order model which indicating that the prevailing process is chemisorption, through sharing of electrons between the adsorbate and the adsorbent surface [29]. Moreover, the obtained results in Tables 12 , 13 and 14 shown that the maximum adsorption (qe) was observed for fluoride ions (2628 mg/ g), followed by phosphate ions (944 mg/ g), then TSS (554 mg/ g), and the lowest were iron ions (115 mg/ g), and COD (244 mg/ g).

Adsorption reaction models, such as first- and second-order kinetic models, are assumed that the rate of adsorption is controlled by the adsorption rate of the solute on the adsorbent surface, and both intraparticle diffusion and external mass transport can be neglected [30]. Accordingly, intra-particle diffusion model has been applied to figure out the adsorption mechanism. The correlation coefficient of the models has been used to predict the best fit models.

In Figure 13, the graphical representations are linear, but none passes through the origin, which indicates that both diffusion mechanisms are involved in the sorption processes for iron, fluoride, phosphate, and COD and TSS. From the Figure it is clear that there are two line segments (Multi linearity) for each sorbent which indicated that iron, fluoride, phosphate, and COD and TSS sorption process is controlled by multiple mechanisms [31]. Each linear segment represents a controlling mechanism. The first part is generally associated with film diffusion (or chemical reaction), and the following second linear part represents intra particle diffusion into the porous structure of the sorbent [32]. This means that the adsorption proceeds via a complex mechanism consisting of both film adsorption and intraparticle transport within the pores of activated charcoal.

The confirmation of efficient adsorption by the activated carbon could be verified through the given FT-IR spectra (Figure 14) and SEM (Figure 15) of the spent adsorbent.

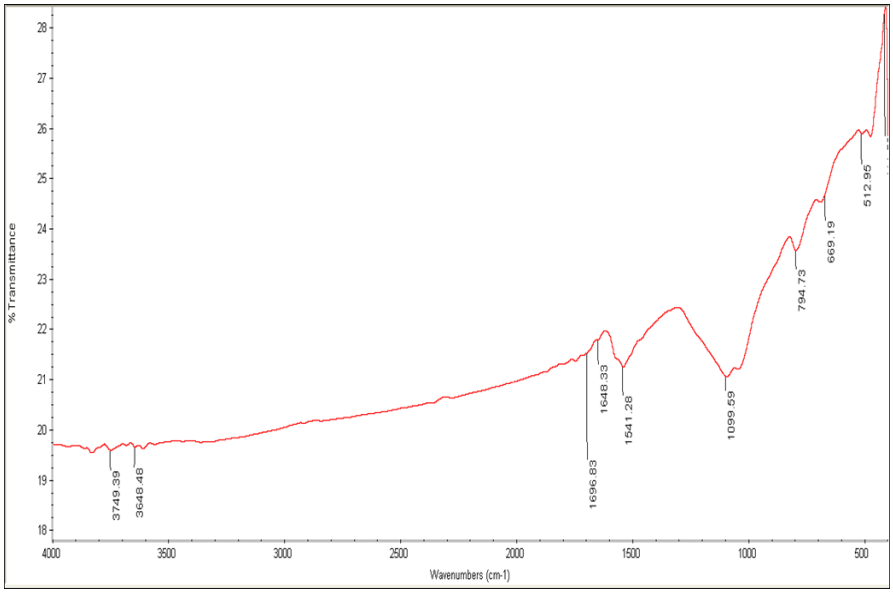

Figure 14 : FT-IR spectrums of activated carbon species after adsorption process.

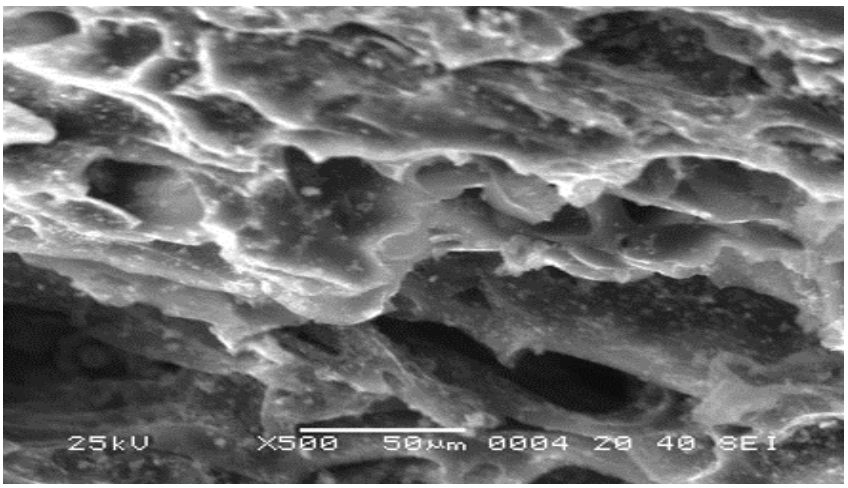

Figure 15 : SEM image of activated carbon species after adsorption process**.**

FTIR spectra of the activated carbon after adsorption process take place a reduction in the bands intensity especially; the strong band at 3648-3749 cm−1 as well as the peak at 1541 cm−1 and 1091 cm−1. The Figure clear also the disappearance of several bands such as the bends in the range 1696-1747 cm−1, this confirming the adsorption process. The same confirmation has been clearly presented by SEM image (Figure 15). From the Figure it is indicated that the surface morphology of the activated carbon changed clearly after the adsorption process, where the surface morphology of AC after adsorption, demonstrates compacted aggregates. Moreover, the surface porosity of the activated carbon declined significantly after adsorption process which confirming the wastes adsorption.

Sorption Thermodynamics

The proper assessment of the thermodynamic parameters is considered important to determine the effect of temperature on the sorption capacity, and to provide information regarding the effect of sorption process on the inherent energy and structure changes of the adsorbent [33]. The thermodynamic parameters of iron, fluoride, phosphate, and COD and TSS sorption from wastewater stream sample onto activated charcoal were determined from the temperature dependent distribution coefficient (Kd) using Van't Hoff equation [31] (eq. 1). In addition,

The Gibbs free energy change ΔG and the entropy change, ΔS could be calculated from equations eq.2 and eq.3 respectively.

The experimental results obtained in Tables 6 and 7 were used to calculate the distribution coefficient (Kd) for iron, fluoride, phosphate, COD and TSS sorption, as shown in Tables (22-23- 24-25-26).

Table 22: The values of Kd for iron sorption using activated charcoal relative to the temperature values.

Temperature (°C)	1000/ T (K)	Ce	K_d	log Kd
25	3.36	204	341.9	2.53
35	3.25	209	325.8	2.51
45	3.14	218	296.8	2.47
55	3.05	228	264.5	2.42
65	2.96	237	235.5	2.37

Table 23 : The values of Kd for fluoride sorption using activated charcoal relative to the temperature values.

Temperature (°C)	1000/ T (K)	Ce	K_d	log Kd
25	3.36	820	758.8	2.88
35	3.25	835	754.4	2.88
45	3.14	890	738.2	2.87
55	3.05	915	730.9	2.86
65	2.96	944	722.4	2.86

Table 24 : The values of Kd for phosphate sorption using activated charcoal relative to the temperature values.

Temperature (°C)	1000/ T (K)	Ce	K_d	log Kd
25	3.36	217	806	2.91
35	3.25	225	799.1	2.9
45	3.14	241	784.8	2.89
55	3.05	259	768.8	2.89
65	2.96	276	753.6	2.88

Table 25 : The values of K_d for COD sorption using activated charcoal relative to the temperature values.

Temperature (°C)	1000/ T (K)	Ce	K_d	log Kd
25	3.36	53	817.2	2.91
35	3.25	62	786.2	2.9
45	3.14	81	720.7	2.86
55	3.05	98	662.1	2.82
65	2.96	115	603.4	2.78

Table 26: The values of K_d for TSS sorption using activated charcoal relative to the temperature values.

Temperature (°C)	1000/ T (K)	C_e	K_d	log K_d
25	3.36	74	878.7	2.94
35	3.25	78	872.1	2.94
45	3.14	87	857.4	2.93
55	3.05	97	841	2.92
65	2.96	105	827.9	2.92

The values of enthalpy change (ΔH) and entropy change (ΔS) for the adsorption process are determine from the slope and intercept for the plot of logK_d versus 1/T as shown in Figure 16.

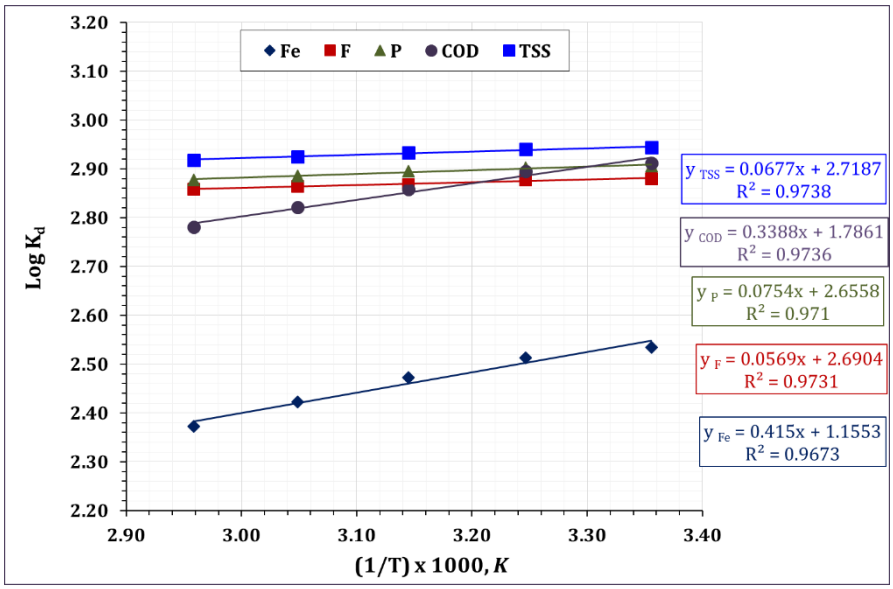

Figure 16: Variation of log Kd with 1/T for iron, fluoride, phosphate, and COD and TSS sorption from wastewater using activated charcoal.

The thermodynamic parameters of iron, fluoride, phosphate, and COD and TSS adsorption from wastewater onto activated charcoal are given in Table 27.

Table 27: Thermodynamic parameters for iron, fluoride, phosphate, and COD and TSS sorption from wastewater using activated charcoal.

	ΔG (kJ/mol)					**ΔH**	**ΔS**
	25 °C	**35 °C**	**45 °C**	**55 °C**	**65 °C**	(kJ/mol)	(J/mol K)

Fe	-14.4	-14.8	-15	-15.2	-15.3	-7.9	22.2
F	-16.4	-16.9	-17.4	-18	-18.5	-1.1	52.3
P	-16.6	-17.1	-17.6	-18.1	-18.6	-1.4	51.6
COD	-16.6	-17.1	-17.4	-17.7	-18	-6.5	34.5
TSS	-16.8	-17.3	-17.8	-18.4	-18.9	-1.3	52.9

The obtained data in Table 3.52 show the enthalpy change (ΔH) values were negative for iron, fluoride, phosphate, and COD and TSS sorption from wastewater, which indicated the exothermic nature of the adsorption onto activated charcoal. This means that, the total energy absorbed in bond breaking is less than the total energy released in bond making between adsorbate and adsorbent, resulting in the release of extra energy in the form of heat. Therefore ΔH will be negative [34]. Moreover, the magnitude of ΔH of iron, fluoride, phosphate, and COD and TSS sorption process is less than 20 kJ mol-1, which means that the sorption is physical sorption process. The change in entropy (ΔS) was positive for iron, fluoride, phosphate, and COD and TSS, indicating the entropy of the system increased during the adsorption process. However, it should also be noted that the entropy of the universe (including the system and the surroundings) might increase because the adsorption reaction was not an isolated process.

The negative values of free energy change (ΔG) for iron, fluoride, phosphate, and COD and TSS adsorption process clear that the adsorption process onto activated charcoal was a spontaneous process [35]. This behavior could be as a result of that by increase the temperature, iron, fluoride, phosphate, and COD and TSS species are readily dehydrated and thereby their sorption becomes more favorable [34]. The absolute values of ΔG for iron, fluoride, phosphate, and COD and TSS sorption onto activated charcoal were smaller than 20 kJ mol-1, which confirm that the sorption process is consistent with electrostatic interaction between sorption sites and the metal ion (physisorption process) [34].

Sorption Process Investigation

According to the above-mentioned results- for Fe, F and P ions and COD and TSS sorption rom wastewater stream onto activated charcoal it is clear that; the sorption efficiency for Fe, F and P ions and COD and TSS was 34.2, 75.4, 80.4, 81.4, and 87.5% respectively according to the following experimental conditions; shaking time of 30 min, solution pH of 4, room temperature, and sorbent amount of addition of 2.0 g/ L.

Based on the aforementioned investigations, a process for wastewater treatment batch wise with activated charcoal was developed. In this respect, 1.0 liters of wastewater sample was treated with 2.0 g of activated charcoal for 30 min at room temperature. Subsequent filtration was occurred. The chemical analysis of wastewater sample before and after treatment process is given in Table 28. From the Table, it is clear that activated carbon has also remarkable effect on the concentration of turbidity, conductivity, TDS as well as sulfate in the wastewater sample.

Table (28): Chemical analysis of the wastewater working sample before and after treatment with activated charcoal.

Components	Before treatment	After treatment	Sorption Efficiency (%)
	Concentration		
pH	3.4	4	-
Turbidity (NTU)	150	25	83.3
Conductivity (µmho/cm)	10560	4690	55.6
TSS (mg/L)	610	79	87.0
TDS (mg/L)	13200	7680	41.8
COD (ppm)	290	57	80.3
Total hardness (ppm)	6500	3610	44.5
P (ppm)	1120	228	79.6
SiO_2 (ppm)	1751	1220	30.3
SO_4 (ppm)	512	170	66.8
Cl^-	205	48	76.6
F	3400	842	75.2
Fe	310	206	33.5

REFERENCES

1. Neumann RP, Hilty M, Xu B, Usemann J, Korten I, Mika M, et al. Nasal microbiota and symptom persistence in acute respiratory tract infections in infants. ERJ Open Research. 2018;4(4):00066.
2. Bosch AATM, Biesbroek G, Trzcinski K, Sanders EAM, Bogaert D. Viral and bacterial interactions in the upper respiratory tract. PLoS Pathogens. 2013;9(1):1003057.
3. Chochua S, D'acremont V, Hanke C, Alfa D, Shak J, Kilowoko M, et al. Increased nasopharyngeal density and concurrent carriage of Streptococcus pneumoniae, Haemophilus influenzae, and Moraxella catarrhalis are associated with pneumonia in febrile children. Plos One. 2016;11(12):0167725.
4. Wang L, Fu J, Liang Z, Chen J. Prevalence and serotype distribution of nasopharyngeal carriage of Streptococcus pneumoniae in China: a meta-analysis. BMC Infect Dis. 2017;17(1):765.
5. Perez AC, Murphy TF. A Moraxella catarrhalis vaccine to protect against otitis media and exacerbations of COPD: An update on current progress and challenges. Hum Vaccin Immunother. 2017;13(10):2322-2331.
6. Chao Y, Marks LR, Pettigrew MM, Hakansson AP. Streptococcus pneumoniae biofilm formation and dispersion during colonization and disease. Front Cell Infect Microbio. 2015;13(4):194.
7. Marom T, Nokso-Koivisto J, Chonmaitree T. Viral-bacterial interactions in acute otitis media. Curr Allergy Asthma Rep. 2012;12(6):551-558.
8. de Steenhuijsen Piters WAA, Heinonen S, Hasrat R, Bunsow E, Smith B, Chaussabel D, et al. Nasopharyngeal Microbiota, Host Transcriptome, and Disease Severity in Children With Respiratory Syncytial Virus Infection-PubMed. National Center for Biotechnology Information. Am J Respir Crit Care Med. 2016;194(9):1104-1115.
9. Schuez-Havupalo L, Toivonen L, Karppinen S, Kaljonen A, Peltola V. Daycare attendance and respiratory tract infections: a prospective birth cohort study. BMJ Open. 2017;7(9):e014635.
10. Koliou MG, Andreou K, Lamnisos D, Lavranos G, Lakovides P, Economou C, et al. Risk factors for carriage of Streptococcus pneumoniae in children. BMC Pediatrics. 2018;18(1):144.
11. Miller JM, Binnicker MJ, Campbell S, Carroll CK, Chapin CK, Gilligan HP, et al. A guide to utilization of the microbiology laboratory for diagnosis of infectious diseases: 2018 update by the Infectious Diseases Society of America and the American Society for Microbiologya. 2018;67(6):813-816
12. Hendaus M, Jomha F, Alhammadi A. Virus-induced secondary bacterial infection: a concise review. Ther Clin Risk Manag. 2015;11(1):1265-1271
13. Goldblatt D, Scadding GK, Lund VJ, Wade AM, Turner MW, Pandey JP. Association of Gm allotypes with the antibody response to the outer membrane proteins of a common upper respiratory tract organism, Moraxella catarrhalis. J Immunol. 1994;153(11):5316-5320.

14. Torfason EG, Reimer CB, Keyserling HL. Subclass restriction of human enterovirus antibodies. J Clin Microbiol. 1987;25(8):1376-1379.